



Virginia Commonwealth University
VCU Scholars Compass

Electrical and Computer Engineering Publications

Dept. of Electrical and Computer Engineering

2004

Determination of the carrier concentration in InGaAsN/GaAs single quantum wells using Raman scattering

Patrick A. Grandt

University of Arkansas - Main Campus

Aureus E. Griffith

University of Arkansas - Main Campus

M. O. Manasreh

University of Arkansas - Main Campus, manasreh@engr.uark.edu

See next page for additional authors

Follow this and additional works at: http://scholarscompass.vcu.edu/egre_pubs

 Part of the [Electrical and Computer Engineering Commons](#)

Grandt, P.A., Griffith, A.E., Manasreh, M.O., et al. Determination of the carrier concentration in InGaAsN/GaAs single quantum wells using Raman scattering. *Applied Physics Letters*, 85, 4905 (2004). Copyright © 2004 AIP Publishing LLC.

Downloaded from

http://scholarscompass.vcu.edu/egre_pubs/131

This Article is brought to you for free and open access by the Dept. of Electrical and Computer Engineering at VCU Scholars Compass. It has been accepted for inclusion in Electrical and Computer Engineering Publications by an authorized administrator of VCU Scholars Compass. For more information, please contact libcompass@vcu.edu.

Authors

Patrick A. Grandt, Aureus E. Griffith, M. O. Manasreh, D. J. Friedman, S. Doğan, and D. Johnstone

Determination of the carrier concentration in InGaAsN/GaAs single quantum wells using Raman scattering

Patrick A. Grandt, Aureus E. Griffith, and M. O. Manasreh^{a)}

Department of Electrical Engineering, 3217 Bell Engineering Center, University of Arkansas, Fayetteville, Arkansas 72701

D. J. Friedman

National Renewable Energy Laboratory, 1617 Cole Boulevard, Golden, Colorado 80401

S. Doğan and D. Johnstone

Virginia Commonwealth University, Department of Electrical Engineering, 601 W. Main Street, P. O. Box 843072, Richmond, Virginia 23284-3072

(Received 18 June 2004; accepted 20 September 2004)

Raman scattering from longitudinal optical phonon-plasmon coupled mode was observed in a series of InGaAsN/GaAs single quantum well samples grown by metalorganic vapor phase epitaxy. The phonon-plasmon mode spectra were fitted with the dielectric constant function based on Drude model that contains contributions from both lattice vibrations and conduction electrons. The carrier concentration is calculated directly from the plasmon frequency, which is obtained from the fitting procedure. An empirical expression for the electron concentration, $[n]$, in InGaAsN/GaAs samples is determined as $[n] \approx \{2.35 \times 10^{16}(\omega_m - 502)\} \text{cm}^{-3}$, where ω_m is the peak of the upper frequency branch, L_+ , of the phonon-plasmon mode measured in unit of cm^{-1} . The phonon-plasmon coupled mode was also investigated in rapid thermally annealed samples. © 2004 American Institute of Physics. [DOI: 10.1063/1.1823014]

Dilute nitride materials such as InGaAsN have been the subject of intense investigation for their applications in multijunction photovoltaic¹⁻³ and optoelectronic devices operating at 1.3 and 1.5 μm .⁴⁻⁶ This is due, in part, to the large band gap bowing factor resulting from nitrogen incorporation in the material. For example, the addition of 2% nitrogen causes the band gap to decrease by about 0.4 eV (see, for example, Ref. 7). The ability to vary the band gap of the alloy material in a wide range by optimizing the nitrogen content provides means to tailor the material properties for the desired device applications.

The determination of the conduction electrons concentration in diluted nitrides is very important for device fabrication. Hall effect is typically the method used for measuring the carrier concentration in semiconductors, which requires the fabrication of ohmic contacts. It is possible, however, to determine the carrier concentration in polar semiconductor materials using Raman scattering without the need of ohmic contacts. This is because the collective oscillation (plasmon) of free carriers can interact with the longitudinal optical (LO) phonons through the longitudinal electric fields and form an LO-plasmon coupled (LOPC) mode. This mode was first demonstrated in GaAs bulk material⁸ and had been recently reported in *n*-type GaN thin films.⁹⁻¹¹

The Raman scattering intensity, $I(\omega)$, is related to the dielectric constant according to the following relation (see, for example, Ref. 12):

$$I(\omega) \propto \text{Im} \left[-\frac{1}{\epsilon(\omega)} \right], \quad (1)$$

where $\epsilon(\omega)$ is the dielectric function consisting of phonon and plasmon contributions and is given by

$$\epsilon(\omega) = \epsilon_\infty \left(1 + \frac{\omega_L^2 - \omega_T^2}{\omega_T^2 - \omega^2 - i\omega\Gamma} - \frac{\omega_p^2}{\omega^2 - i\omega\gamma} \right), \quad (2)$$

where ϵ_∞ is the high frequency dielectric constant and is approximately taken as the square of the refractive index at the probe laser wavelength used (1064 nm), ω_L is the LO phonon frequency (291 cm^{-1}), ω_T is the transverse optical (TO) phonon frequency (268 cm^{-1}), Γ is the phonon damping rate, γ is plasmon damping rate, and ω_p is the plasmon frequency given by

$$\omega_p^2 = \frac{ne^2}{\epsilon_0 \epsilon_\infty m^*}, \quad (3)$$

where n is the carrier concentration, e is the electric charge, ϵ_0 is permittivity of space, and m^* is the electron effective mass. Notice that LO and TO phonon frequency were obtained from the Raman measurements as shown in Fig. 1. These frequencies varied slightly from sample to sample, but they are in good agreement with the frequencies reported¹³ for InGaAsN. Furthermore, the measured phonon frequencies are slightly smaller than those reported for bulk GaAs materials.¹⁴ The LOPC mode splits into two modes known as L_+ and L_- branches. These two branches are approximately obtained by setting $\Gamma = \gamma = 0$ and solve Eq. (2) for $\epsilon(\omega) = 0$, which yields

$$L_\pm = \frac{1}{\sqrt{2}} [(\omega_L^2 + \omega_p^2) \pm \sqrt{(\omega_L^2 + \omega_p^2)^2 - 4\omega_T^2\omega_p^2}]^{1/2}. \quad (4)$$

The GaAs/InGaAsN/GaAs single quantum well samples were grown by atmospheric-pressure metalorganic vapor phase epitaxy at 570 °C on semi-insulating GaAs oriented 2° from (100) to (110). A typical size of the substrate is 1 cm × 2 cm. Trimethylgallium, trimethylindium, arsine, and dimethylhydrazine (DMH) were used as precursors. The growth rate was 5 $\mu\text{m}/\text{h}$ for the InGaAsN active layers. The

^{a)} Author to whom correspondence should be addressed; electronic mail: manasreh@engr.uark.edu

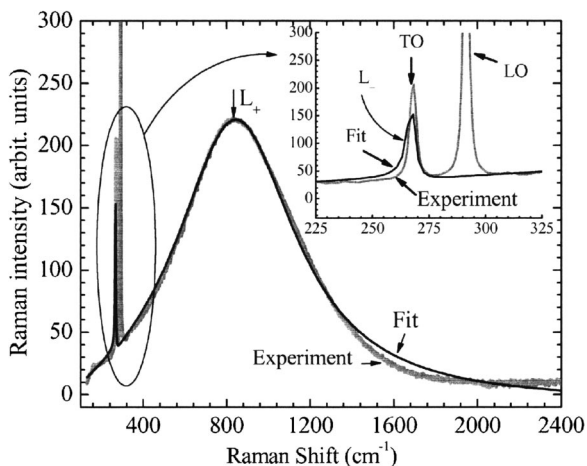


FIG. 1. A Raman scattering spectrum obtained for an InGaAsN/GaAs single quantum well sample (gray line). The spectrum shows the LO, TO and the L_+ branches of the LOPC mode. The solid black line is the result of the fitting analysis using Eq. (1), which shows both the L_+ and L_- branches of the LOPC mode. The inset is the expansion of the spectral region in the vicinity of LO and TO phonon modes.

N content was changed for the various samples by varying the DMH source flow rate and the In mole fraction was approximately 7% for all samples. The InGaAsN active layers were 100 Å thick, and were clad on both sides by n -type GaAs doped with silicon from disilane precursor with doping level on the order of mid 10^{18} cm^{-3} . The cladding layers varied in thickness. Several of these samples were used in a previous photoluminescence study¹⁵ where the indium and the nitrogen contents were reported. The Raman scattering spectra were recorded at room temperature using a Fourier-transform spectrometer in conjunction with a yttrium-aluminum-garnet laser and an optics transfer attachment.

A typical Raman scattering spectrum of LOPC mode in InGaAs/GaAs single quantum well is shown in Fig. 1 as the gray spectrum. This spectrum was fitted with Eq. (1) and the result is shown as the thin black line. The fitting procedure reveals both L_+ and L_- . The L_- region along with the LO and TO phonon modes are re-plotted in the figure inset for clarity. The plasma frequency, ω_p , was used as one of the fitting parameters. The fitting procedure, illustrated in Fig. 1, was repeated for several samples, from which L_+ and ω_p were obtained. The frequency maximum of L_+ branch was obtained for the samples and plotted as a function of the plasmon frequency, as shown in Fig. 2. Equation (4) is also plotted in this figure (solid lines) along with the LO and TO phonon modes (dashed lines).

The carrier concentration, $[n]$, is calculated from the plasmon frequency according to Eq. (3) for several samples. The frequency maximum, ω_m , of the LOPC mode upper branch is plotted as a function of the carrier concentration, as shown in Fig. 3. The solid line is the result of the linear fit of the data from which the following expression is obtained: $[n]=2.35 \times 10^{16}(\omega_m - 502) \text{ cm}^{-3}$. This expression can be used to obtain the carrier concentration directly from the peak of L_+ mode, which is measured directly by Raman scattering in unit of cm^{-1} , as shown in Fig. 1.

Another test of the LOPC mode in InGaAsN/GaAs single quantum well samples is the thermal annealing. Both furnace annealing and rapid thermal annealing (RTA) have a drastic effect on the carrier concentration in semiconductor including diluted nitrides. Several InGaAsN/GaAs

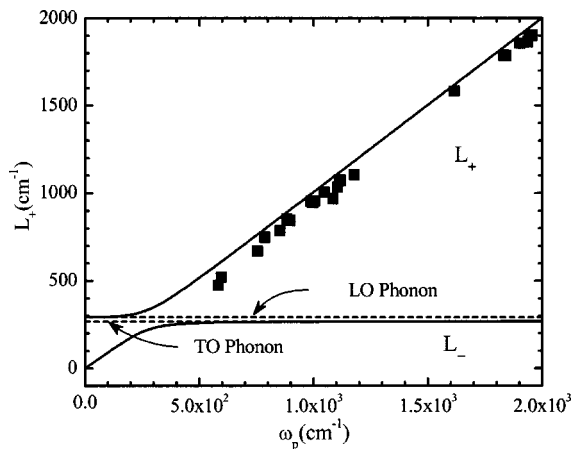


FIG. 2. A plot of the L_+ mode as a function of the plasmon frequency for a series of InGaAsN/GaAs single quantum well samples (solid squares). The plasmon frequency, ω_p , was obtained from fitting the LOPC mode in the samples. The solid lines are plots of L_+ and L_- given by Eq. (4). The dashed lines represent the LO and TO phonon frequencies.

single quantum well samples were annealed using an RTA setup. A typical result of the RTA effect on the LOPC mode is shown in Fig. 4, where the Raman scattering spectra (gray lines) are recorded for two pieces cut from the same wafer, of which one was annealed at 900°C for 30 s and the other was unannealed. It is clear from this figure that a large blue-shift is observed for the LOPC mode in the annealed sample. This behavior is observed in all annealed samples. Both spectra were fitted using Eq. (1) and the fitted lines are displayed as the thin black lines. The plasmon frequencies obtained from the fitting procedure are 1053 and 2054 cm^{-1} for the unannealed and annealed samples, respectively, with accuracy less than 0.5% as obtained from the fitting results. The corresponding carrier concentrations are $1.0 \times 10^{19} \text{ cm}^{-3}$ for the unannealed sample and $3.9 \times 10^{19} \text{ cm}^{-3}$ for the annealed sample, an increase of a factor of 3.9. A plausible explanation of the increase of the carrier concentration in the annealed sample is that many of the defects, imperfections, and traps in the structure are annealed out releasing the electrons to the conduction band. It is obvious that the increase of the carrier concentration causes the blue-shift of the LOPC mode, which is demonstrated experimentally in Fig. 4.

It is noted that the full width at half maximum of the spectrum obtained for the annealed sample in Fig. 4 is larger

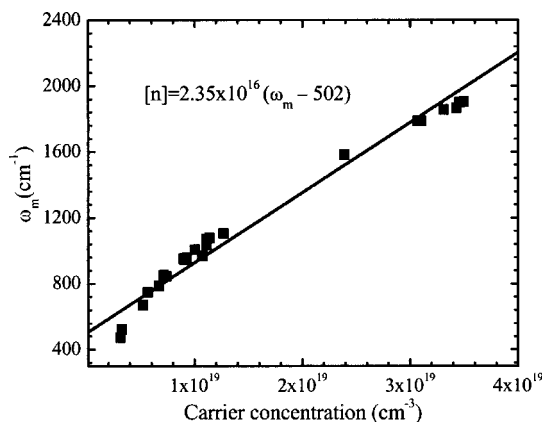


FIG. 3. The frequency maximum, ω_m , of L_+ branch as a function of the carrier concentration obtained from the data in Fig. 2. The solid line is a first order linear fit of the data.

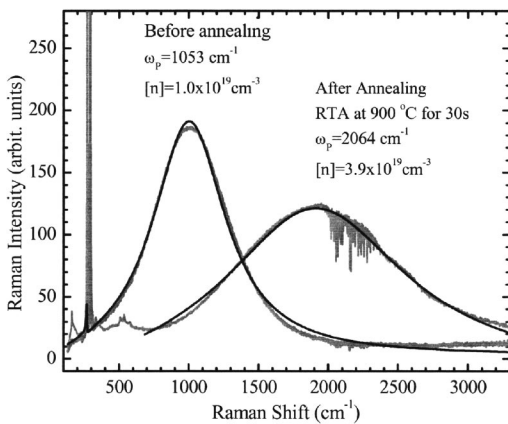


FIG. 4. Rapid thermal annealing effect on the LOPC mode in InGaAsN/GaAs single quantum well. The gray lines represent the Raman scattering spectra obtained for unannealed and annealed samples cut from the same wafer. The thin black lines represent the results of the fitting analysis.

than that of the unannealed sample. This is translated into a larger plasmon damping rate, γ , which is also used in the fitting analysis. The γ values obtained for the Raman spectra in Fig. 4 are 634 and 1549 cm^{-1} before and after annealing, respectively, with accuracy less than 0.5% as obtained from fitting results. The plasmon damping rate is related to the carrier drift mobility, μ , through the following relation: $\mu = e/(m^* \gamma)$. Thus, the carrier mobility in the annealed sample is about a factor of 2.44 smaller than that of the unannealed sample.

One possible explanation of the reduction of the mobility is the electron-electron scattering, which is significant for systems with carrier concentration larger than 10^{18} cm^{-3} (see, for example, Refs. 19–21). The electron-electron scattering increases as the electron concentration is increased. Hence, the carrier drift mobility decreases as the electron-electron scattering is increased. The drift mobility values estimated from the plasmon damping rate are ~ 220 and $\sim 90 \text{ cm}^2 \text{ V}^{-1} \text{ s}^{-1}$ for the unannealed and annealed samples, respectively. While the above explanation is a plausible reason, there are other scattering mechanisms that may affect the mobility.

These mobility values are in good agreement with those reported by Young, Geisz, and Coutts.²² The electron effective mass was chosen as $0.067m_0$, which is the effective mass in the bulk GaAs material, in our estimation of the carrier concentration [see Eq. (3)] and the drift mobility. For InGaAsN material, the effective mass is still surrounded by controversy. Recent reports^{23,24} show that the electron effective mass is ranging between $\sim (0.1 \text{ and } 0.5)m_0$, while other reports^{22,25,26} indicate that the electron effective mass is in the range of $\sim (0.004\text{--}0.11)m_0$. Thus, our choice of m^* is in agreement with the latter range.

In conclusion, the Raman scattering from longitudinal optical phonon-plasmon coupled mode is investigated in a series of InGaAsN/GaAs single quantum well samples. A Drude based dielectric constant, which contains contribution from lattice vibrations and plasmon, is used for the line-shape fitting analysis of Raman spectra. The plasmon frequency was extracted from the analysis and used to calculate the electron concentrations in the samples. An empirical ex-

pression for the carrier concentration as a function of the frequency maximum of the LOPC coupled mode upper branch is obtained, which allows one to directly estimate the carrier concentration from the Raman scattering spectra. Rapid thermal annealing reveals a significant increase in the LOPC mode frequency, which is translated to a significant increase in the carrier concentration in the annealed samples. The increase of the carrier concentration in the annealed samples is accompanied by an increase in the plasmon damping rate, which leads to a decrease in the carrier drift mobility.

This work was partially supported by the Air Force Office of Scientific Research Grant No. F49550-04-1-0002.

- ¹D. J. Friedman, J. F. Geisz, S. R. Kurtz, and J. M. Olson, *J. Cryst. Growth* **195**, 409 (1998).
- ²D. J. Friedman, J. F. Geisz, S. R. Kurtz, and J. M. Olson, Second World Conference on Photovoltaic Solar Energy, 6–10 July 1998, Vienna, Austria.
- ³S. R. Kurtz, A. A. Allerman, C. H. Seager, R. M. Sieg, and E. D. Jones, *Appl. Phys. Lett.* **77**, 400 (2000).
- ⁴N. Tansu, J.-Y. Yeh, and L. J. Mawst, *Appl. Phys. Lett.* **83**, 2512 (2003).
- ⁵H. C. Schneider, A. J. Fischer, W. W. Chow, and J. F. Klem, *Appl. Phys. Lett.* **78**, 3391 (2001).
- ⁶X. Yang, J. B. Heroux, M. J. Jurkovic, and W. I. Wang, *Appl. Phys. Lett.* **76**, 795 (2000).
- ⁷W. G. Bi and C. W. Tu, *Appl. Phys. Lett.* **70**, 1608 (1997).
- ⁸A. Mooradian and G. B. Wright, *Phys. Rev. Lett.* **16**, 999 (1966).
- ⁹T. Kozawa, T. Kachi, J. Kano, Y. Taga, and M. Hashimoto, *J. Appl. Phys.* **75**, 1098 (1994).
- ¹⁰H. Harima, in *III-Nitride Semiconductors: Optical Properties I*, edited by M. O. Manasreh and H. X. Jiang (Taylor and Francis, New York, 2002), Vol. 13, Chap. 7.
- ¹¹P. Perlin, J. Camassel, W. Knap, T. Taliercio, J. C. Chervin, T. Suski, I. Grzegory, and S. Porowski, *Appl. Phys. Lett.* **67**, 2524 (1995).
- ¹²M. V. Klein, B. N. Ganguly, and P. J. Colwell, *Phys. Rev. B* **6**, 2380 (1972).
- ¹³G. Leibiger, V. Gottschalch, and M. Schubert, *J. Appl. Phys.* **90**, 5951 (2001).
- ¹⁴V. Swaminathan, A. Jayaraman, J. L. Zilko, and R. A. Stall, *Mater. Lett.* **3**, 325 (1985).
- ¹⁵M. O. Manasreh, D. J. Friedman, W. Q. Ma, C. L. Workman, C. E. George and G. J. Salamo, *Appl. Phys. Lett.* **82**, 514 (2003).
- ¹⁶J. F. Geisz, D. J. Friedman, J. M. Olson, S. R. Kurtz, and B. M. Keyes, *J. Cryst. Growth* **195**, 401 (1998).
- ¹⁷S. R. Kurtz, A. A. Allerman, C. H. Seager, R. M. Sieg, and E. D. Jones, *Appl. Phys. Lett.* **77**, 400 (2000).
- ¹⁸S. Kurtz, J. F. Geisz, D. J. Friedman, J. M. Olson, A. Duda, N. H. Karam, R. R. King, J. H. Ermer, and D. E. Joslin, Proceedings of the 28th IEEE Photovoltaic Specialists Conference, 2000.
- ¹⁹J. Singh, *Electronic and Optoelectronic Properties of Semiconductor Structures* (Cambridge University Press, Cambridge, 2003).
- ²⁰K. F. Brennan, *The Physics of Semiconductors with Applications to Optoelectronic Devices* (Cambridge University Press, Cambridge, 1999).
- ²¹V. V. Mitin, V. A. Kochelap, and M. A. Strosio, *Quantum Heterostructures Microelectronics and Optoelectronics* (Cambridge University Press, Cambridge, 1999).
- ²²D. L. Young, J. F. Geisz, and T. J. Coutts, *Appl. Phys. Lett.* **82**, 1236 (2003).
- ²³Y. Zhang, A. Mascarenhas, H. P. Xin, and C. W. Tu, *Phys. Rev. B* **61**, 7479 (2000).
- ²⁴C. Skierbiszewski, P. Perlin, P. Wisniewski, W. Knap, T. Suski, W. Walukiewicz, W. Shan, K. M. Yu, J. W. Ager, E. E. Haller, J. F. Geisz, and J. M. Olson, *Appl. Phys. Lett.* **76**, 2409 (2000).
- ²⁵C. Skierbiszewski, S. P. Lepkowski, P. Perlin, T. Suski, W. Jantsch, and J. Geisz, *Physica E (Amsterdam)* **13**, 1078 (2002).
- ²⁶P. J. Klar, H. Grüning, W. Heimbrodt, J. Koch, W. Stolz, S. Tomi, and E. P. O'Reilly, *Solid-State Electron.* **47**, 437 (2003).